

Gas/Surface Interaction Models for Porous Media

K. Swaminathan-Gopalan,

Department of Mechanical Science and Engineering, University of Illinois at Urbana-Champaign

A. Borner, J. C. Ferguson,

STC, Computational Physics Branch, NASA Ames Research Center

Prof. K. A. Stephani,

Department of Mechanical Science and Engineering, University of Illinois at Urbana-Champaign

N. N. Mansour

Advanced Supercomputing Division, NASA Ames Research Center

Acknowledgments

This work was performed under the Entry System Modeling Project (M. J. Wright, Project Manager) for the NASA Game Changing Development (GCD) Program and supported by NASA Grant NNX15AU92A.

- Motivation
- Porous Microstructure Analysis (PuMA)
- Surface chemistry framework in PuMA
- GS and PS reactions
- Molecular beam experiments
- Vitreous Carbon (VC) model
- Extension of VC model to FiberForm®
- Effective model for use in CFD
- Summary/Future Work

Motivation

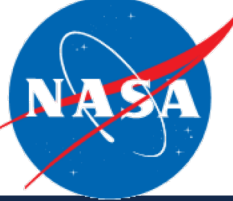


Image credit: NASA

Reusable TPS material considerations:
catalycity, emissivity, toughness

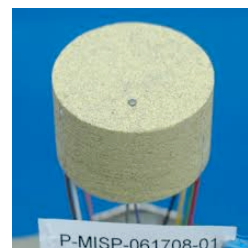


Image credit: NASA

Ablative TPS material considerations:
recession, oxidation, pyrolysis

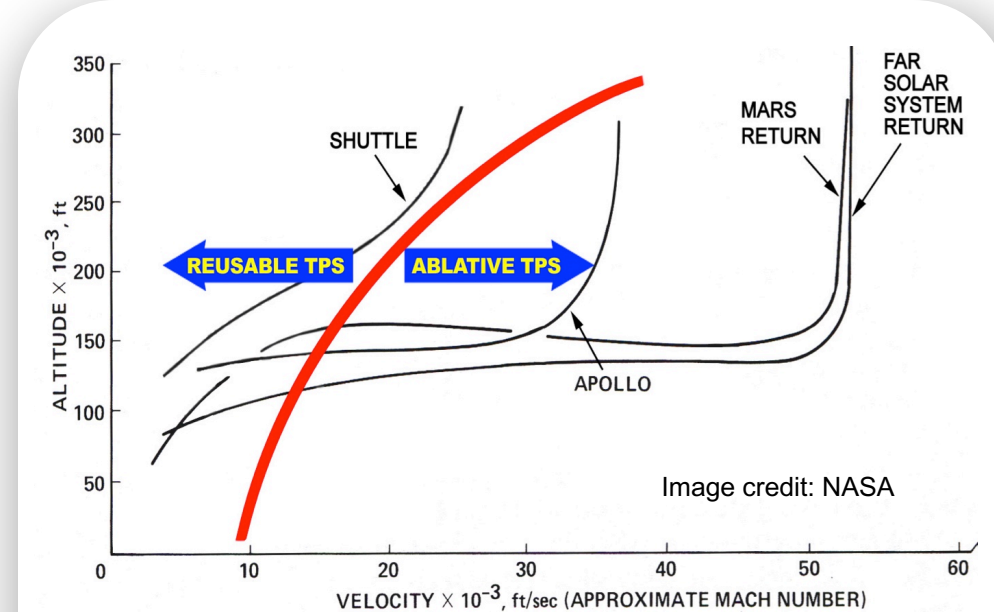
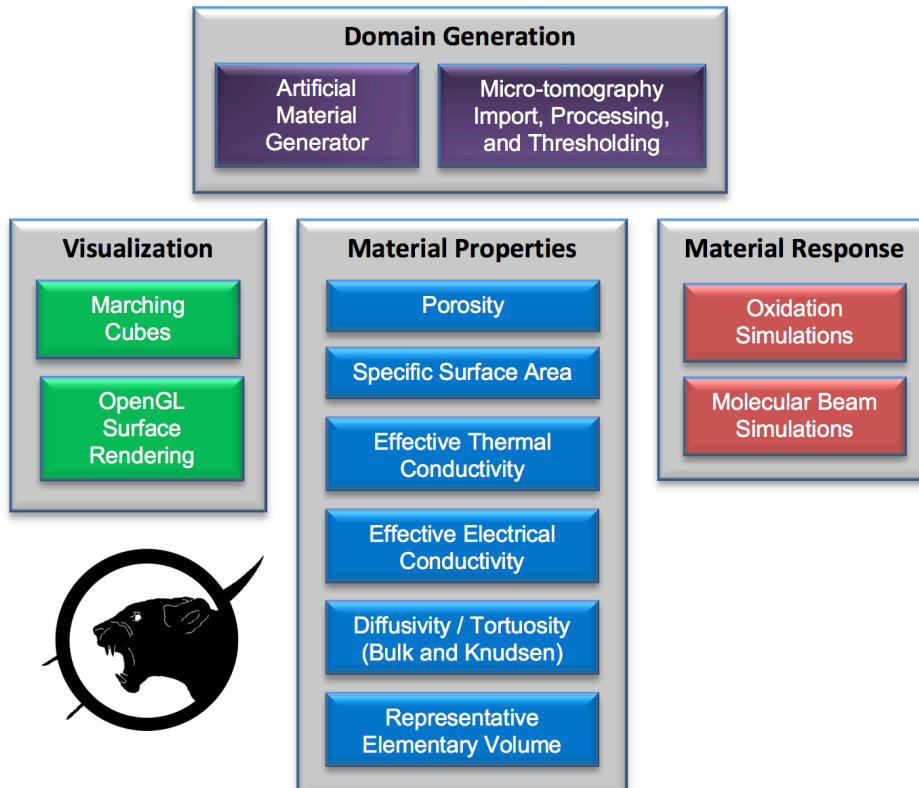


Image credit: NASA

Objectives:

- Characterize carbon surface recession/ablation due to oxidation
- Develop a predictive model of carbon oxidation for use in CFD/DSMC/material response

Porous Microstructure Analysis (PuMA)

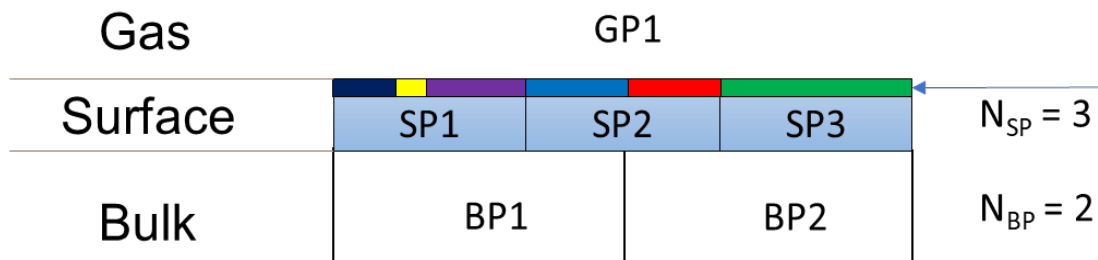


[1] J. C. Ferguson, F. Panerai, A. Borner, N. N. Mansour,
PuMA: the Porous Microstructure Analysis software,
SoftwareX 7 (2018) 81–87.



- Methodology to represent surface sites similar to Marschall, Maclean and Driver [2] for CFD.
- Particles adsorbed (deleted) and desorbed (created), surface element stores adsorbed particle concentration.
- Surface reactions based on concentration within surface element.
- Multiple triangulated elements (like cells) on surfaces
- Langmuir model for surface sites.

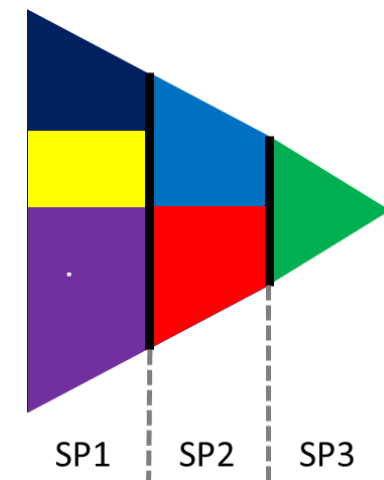
Environments



Phases

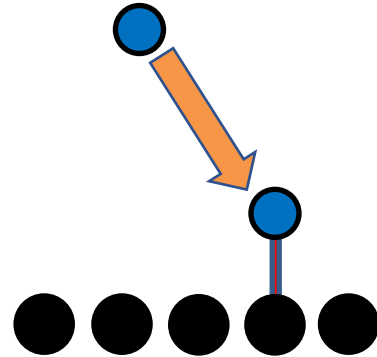
Site Sets

$$\begin{cases} N_{ss, SP1} = 3 \\ N_{ss, SP2} = 2 \\ N_{ss, SP3} = 1 \end{cases}$$

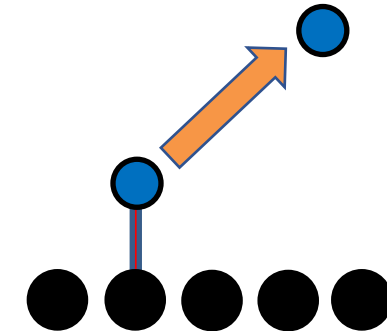


[2] Marschall, J., & MacLean, M. (2011). Finite-rate surface chemistry model, I: Formulation and reaction system examples. AIAA Paper, 3783, 2011.

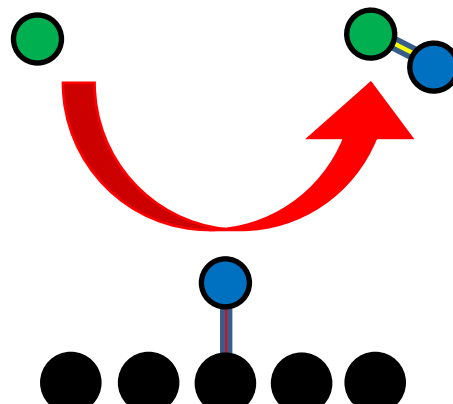
Adsorption



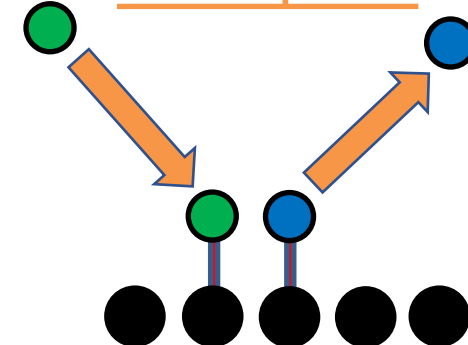
Desorption



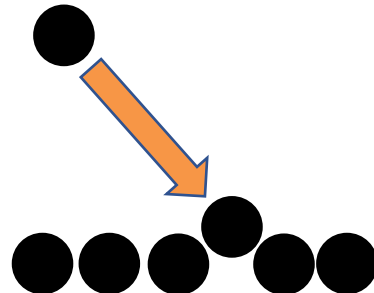
Eley-Rideal



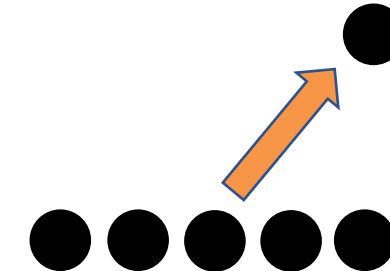
Collision-induced desorption



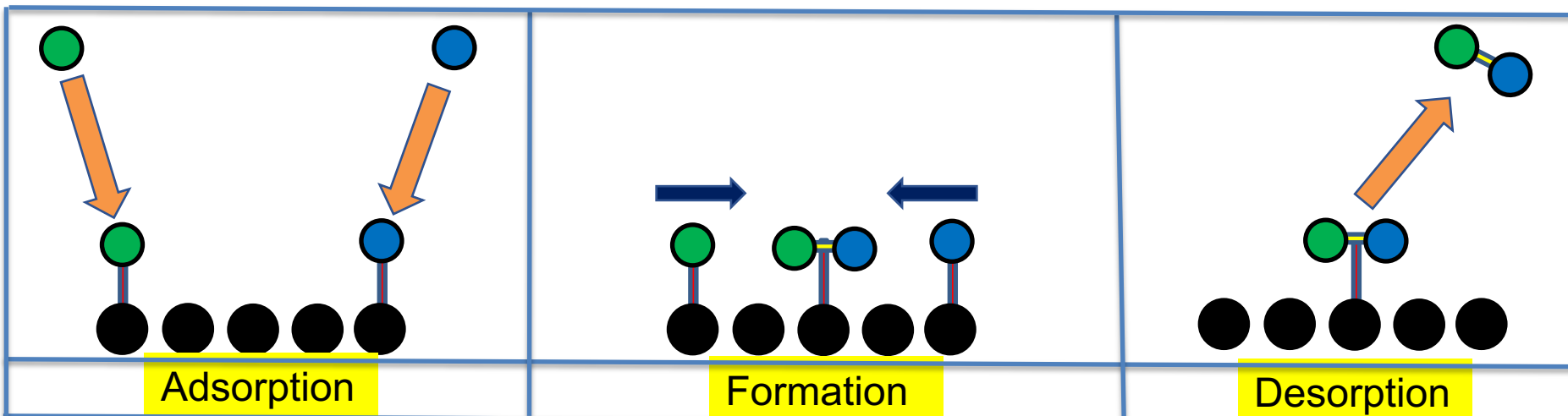
Condensation



Sublimation



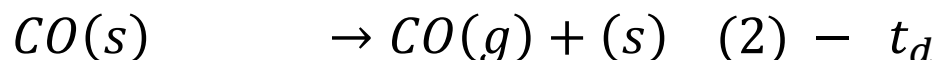
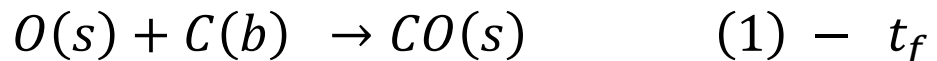
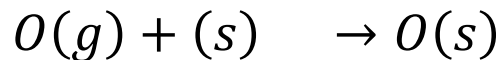
Langmuir-Hinshelwood



Different Types of LH Mechanisms



The Langmuir-Hinshelwood mechanism has two steps – Formation
Desorption



$O(s)$ – Reactant

$CO(s)$ – Intermediate

$CO(g)$ – Product



Time scale of interest = τ

Based on time scale arguments 4 types of LH mechanisms can be defined

1. $t_f \ll \tau$ $t_d \ll \tau$ – Prompt thermal mechanism

2. $t_f \sim \tau$ $t_d \ll \tau$ – LH limited by formation

3. $t_f \ll \tau$ $t_d \sim \tau$ – LH limited by desorption

4. $t_f \sim \tau$ $t_d \sim \tau$ – LH limited by both desorption and formation

List of gas-surface (GS) reactions



- Reactants include both gas-phase and surface species.
- Comprehensive set of reactions – Includes reaction types from thermal regime and hyperthermal energy regime.

| Symbol | Reaction type | Examples |
|--------|-----------------------------|--|
| 1: AA | Associative Adsorption | $O(g) + (s) \rightarrow O(s)$ $O_2(g) + (s) \rightarrow O_2(s)$ |
| 2: DA | Dissociative Adsorption | $O_2(g) + (s) \rightarrow O(s) + O(g)$ $O_2(g) + 2(s) \rightarrow 2O(s)$ |
| 3: DIS | Dissociation | $O_2(g) + (s) \rightarrow 2O(g) + (s)$ $CO_2(g) + (s) \rightarrow 2O(g) + (s) + C(b)$ |
| 4: LH1 | Langmuir-Hinshelwood type 1 | $O(g) + (s) + O(s) \rightarrow O_2(g) + 2(s)$ $O(g) + (s) + C(b) \rightarrow CO(g) + (s)$ |
| 5: LH3 | Langmuir-Hinshelwood type 3 | $O(g) + (s) + O(s) \rightarrow O_2(s) + 2(s)$ $O(g) + (s) + C(b) \rightarrow CO(s) + (s)$ |
| 6: CD | Condensation | $C_3(g) + 3(s) \rightarrow 3C(b) + 3(s)$ |
| 7: ER | Eley-Rideal | $CO(g) + O(s) \rightarrow CO_2(g) + (s)$ |
| 8: CI | Collision Induced | $O(g) + CO(s) \rightarrow CO(g) + O(s)$ $Ar(g) + O(s) \rightarrow Ar(g) + O(g) + (s)$ |

- GS reaction probability computed when gas-phase species hits surface.
- Reaction probability function of:
 - rate constant
 - gas-phase particle properties (energy, angle, etc.)
 - surface conditions (temperature, surface coverage, etc.)

| Reaction type | Sample | Probability |
|--------------------------------------|--|---|
| Adsorption | $A(g) + (s) \longrightarrow A(s)$ | $P = S^\alpha(\theta) = f(S_0, \theta, \alpha)$ [3] |
| | $A_2(g) + (s) \longrightarrow 2A(s)$ | |
| Adsorption mediated reactions: | $A_2(g) + (s) \longrightarrow 2A(g) + (s)$ | $P = P_{ad} * k_{reac}$ |
| Dissociation, LH1, LH3, Condensation | $A(g) + (s) + B(s) \longrightarrow AB(g) + 2(s)$ | $P = P_{ad} * k_{reac} * \frac{N_{B(s)} F_N}{S_p}$ |
| Eley-Rideal | $A(g) + B(s) \longrightarrow AB(g) + (s)$ | $P = 2k_{reac} \frac{N_{B(s)} F_N}{S_p} \frac{1}{v_n}$ [4] |
| Collision Induced | $A(g) + B(s) \longrightarrow A(g) + B(g) + (s)$ | $P = k_{reac} \frac{N_{B(s)} F_N}{S_p} (E_{in})^m \cos^n(\theta)$ [5] |

³ Kisliuk, P. "The sticking probabilities of gases chemisorbed on the surfaces of solids." JPhysChemSolids 3, no. 1-2 (1957): 95-101

⁴ Molchanova, et al. "A detailed DSMC surface chemistry model." In AIP Conference Proceedings, vol. 1628, no. 1, pp. 131-138. AIP, 2014.

⁵ Rettner and Lee. "Dynamic displacement of O₂ from Pt (111): A new desorption mechanism." The JChemPhys 101, no. 11 (1994):

List of pure-surface (PS) reactions



- Pure-surface (PS) reactants include only surface species (adsorbed and bulk).
- Comprehensive set of reactions

| Symbol | Reaction type | Examples |
|--------|-----------------------------|---|
| 1: DS | Desorption | $O(s) \rightarrow O(g) + (s)$ $O_2(s) \rightarrow O_2(g) + (s)$ |
| 2: LH2 | Langmuir-Hinshelwood type 2 | $N(s) + O(s) \rightarrow NO(g) + 2(s)$ $O(s) + C(b) \rightarrow CO(g) + (s)$ |
| 3: LH4 | Langmuir-Hinshelwood type 4 | $N(s) + O(s) \rightarrow NO(s) + (s)$ $O(s) + C(b) \rightarrow CO(s) + (s)$ |
| 4: SB | Sublimation | $3C(b) + 3(s) \rightarrow C_3(g) + 3(s)$ |

- Characteristic time computed between two reactions: Time counter method [5].
- Characteristic time function of
 - reaction rate constant
 - surface conditions (temperature, surface coverage, etc.).

$$\tau_{reac} = \frac{-\log(Rn)}{\nu_{reac}}$$

- Time counter algorithms developed to be independent of dt.

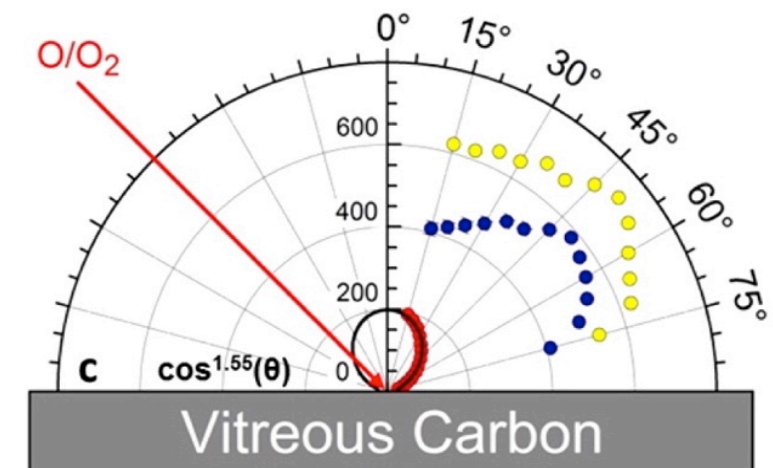
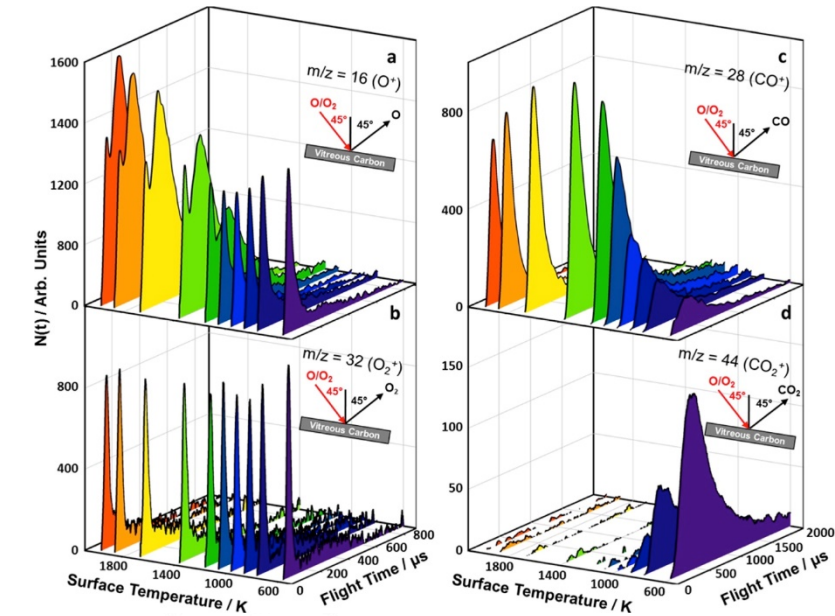
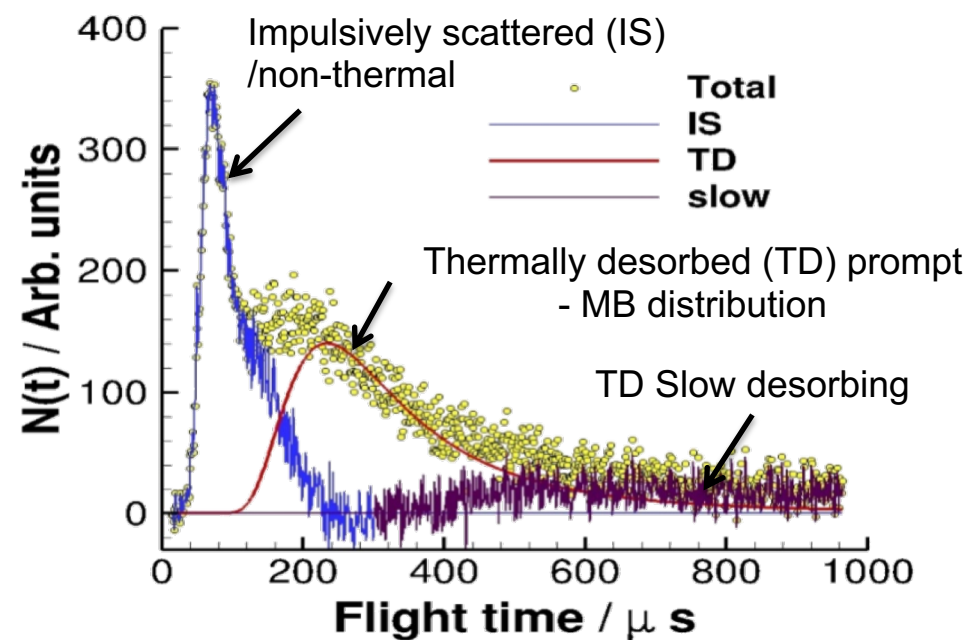
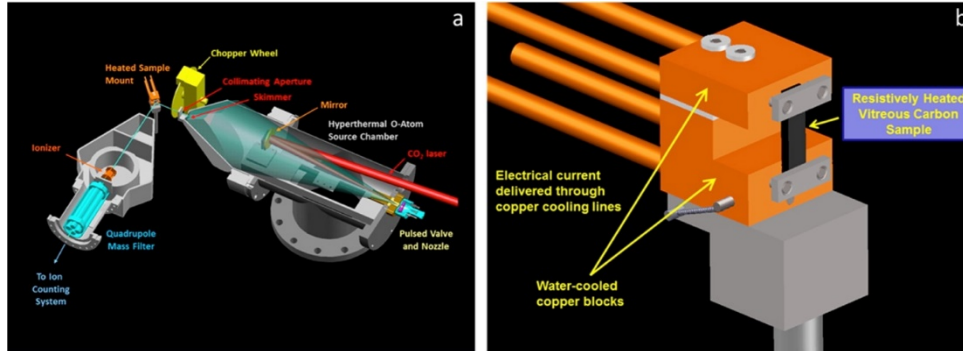
| Reaction type | Sample | Frequency |
|---------------|--|--|
| Desorption | $A(s) \longrightarrow A(g) + (s)$ | $\frac{dn_{A(s)}}{dt} = -k_{reac} n_{A(s)}$ [4] |
| Sublimation | | $\nu_{reac} = k_{reac} N_{A(s)}$ |
| LH-2, LH-4 | $A(s) + B(s) \longrightarrow AB(g) + 2(s)$ | $\frac{dn_{A(s)}}{dt} = \frac{dn_{B(s)}}{dt} = -k_{reac} n_{A(s)} n_{B(s)}$ $\nu_{reac} = k_{reac} N_{A(s)} N_{B(s)} \frac{F_N}{S_p}$ |

⁴ Molchanova, A. N., A. V. Kashkovsky, and Ye A. Bondar. "A detailed DSMC surface chemistry model." In AIP Conference Proceedings, vol. 1628, no. 1, pp. 131-138. AIP, 2014.

Reactive scattering simulation in PuMA



Molecular Beam Experimental Setup [6]



Reprinted with permission from “[6] Murray, V J., et al. *The Journal of Physical Chemistry C* 119.26 (2015): 14780-14796. Copyright 2015. American Chemical Society.

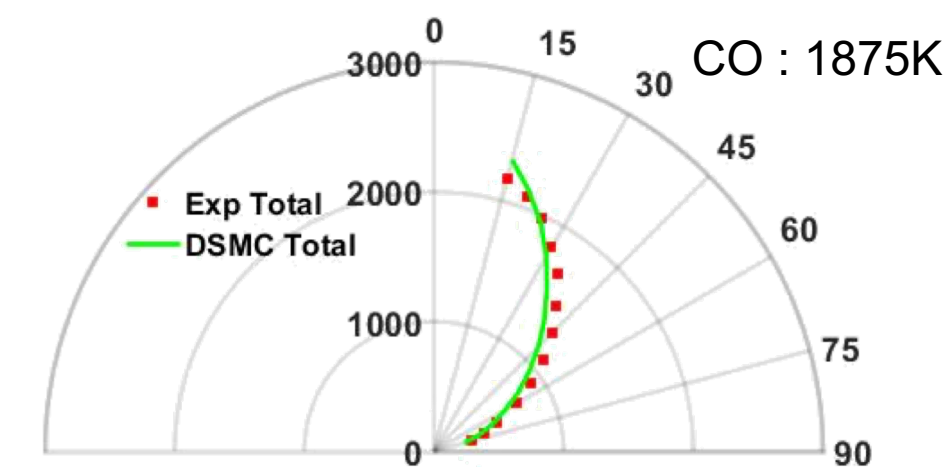
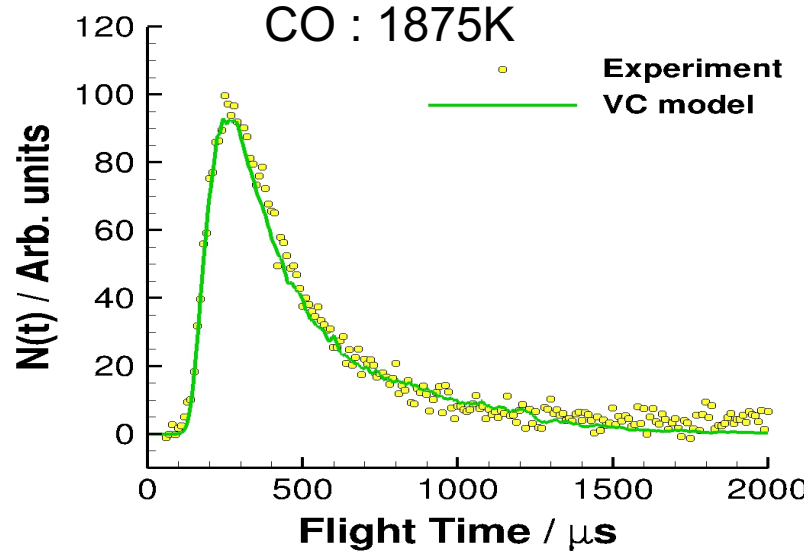
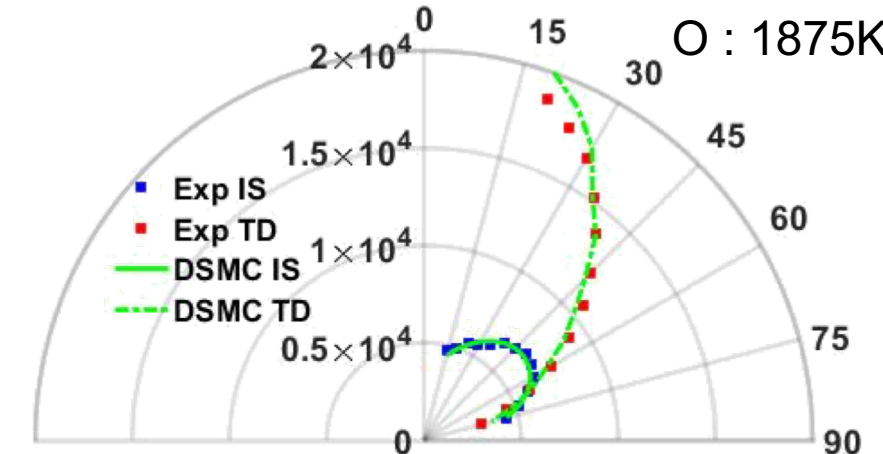
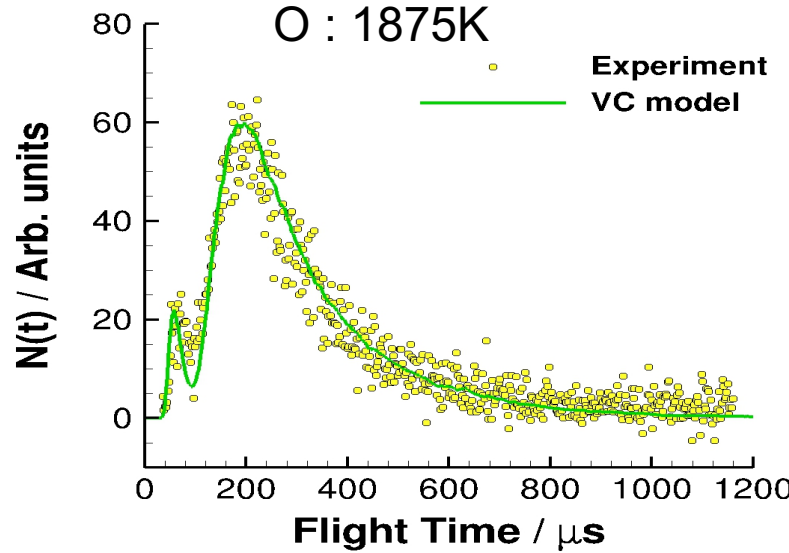
Vitreous Carbon (VC) Oxidation Model [7]

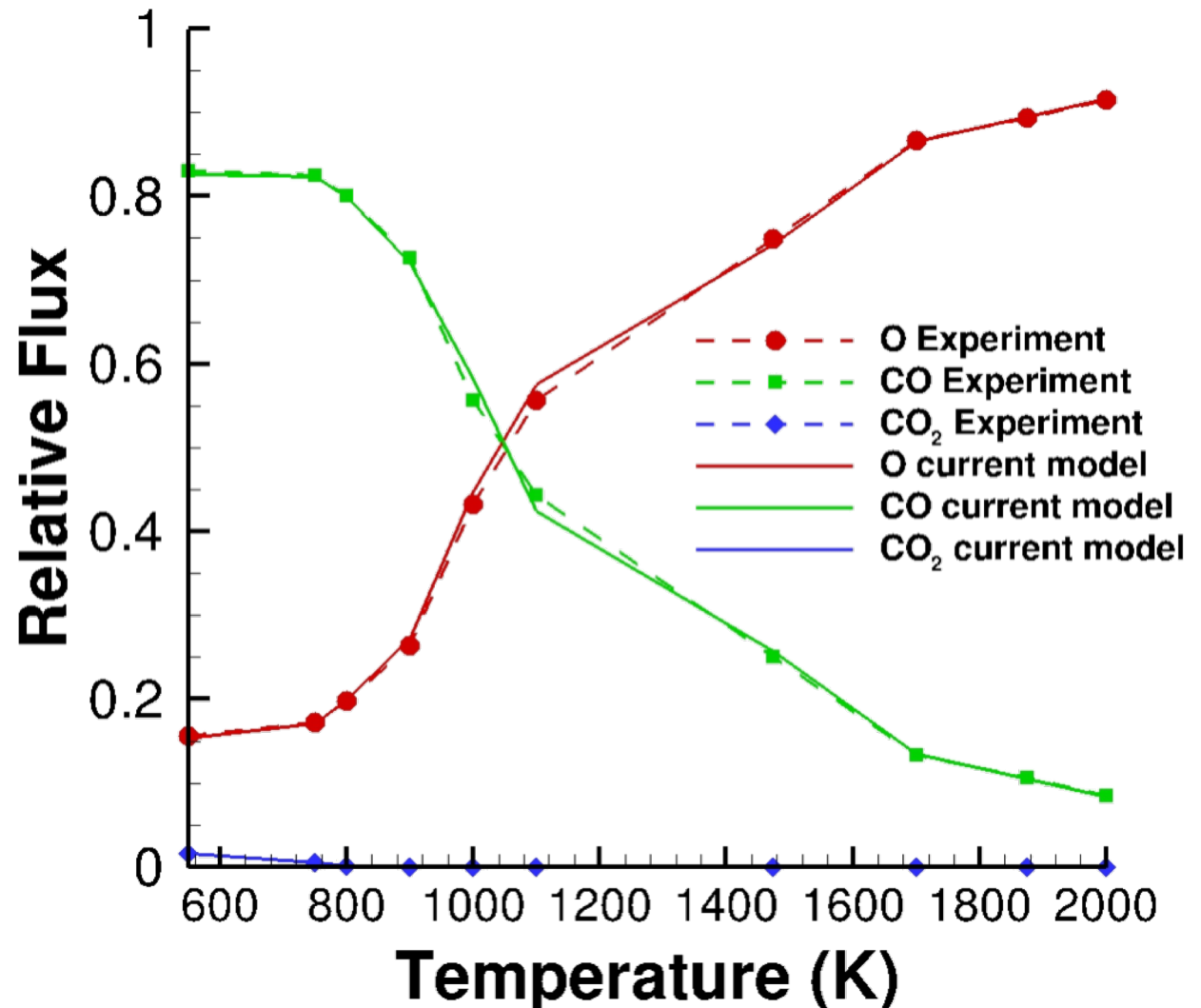


| Type | Mechanisms | Reaction | Rate constant (k) |
|--------------|-------------------------------|---|---|
| Adsorption | Adsorption | $O(g) + (s) \rightarrow O(ads)$ | $\frac{1}{\Phi} * \frac{1}{4} \sqrt{\frac{8k_b T_g}{\pi m}} * 0.85$ |
| | LH1 O formation | $O(ads) \rightarrow O(TD)(g) + (s)$ | $20.9 \exp(-\frac{2449.3}{T_s})$ |
| | LH1 CO formation | $O(ads) + C(b) + O'(ads) \rightarrow CO(g) + (s) + O'(ads)$ | $\frac{1}{\Phi} * 1574.9 \exp(-\frac{6240.0}{T_s})$ |
| | LH1 CO ₂ formation | $O(ads) + O(s) + C(b) + 4O'(ads) \rightarrow CO_2(g) + 2(s) + 4O'(ads)$ | $\frac{1}{\Phi^5} * 536.3 \exp(-\frac{655.6}{T_s})$ |
| GS reactions | LH3 O{a} formation | $O(ads) \rightarrow O\{a\}(s)$ | 1 |
| | LH3 CO{a} formation | $O(ads) + C(b) + O'(ads) \rightarrow CO\{a\}(s) + O'(ads)$ | $\frac{1}{\Phi} * 153.0 \exp(-\frac{4172.8}{T_s})$ |
| | LH3 CO{b} formation | $O(ads) + C(b) + O'(ads) \rightarrow CO\{b\}(s) + O'(ads)$ | $\frac{1}{\Phi} * 71.2 \exp(-\frac{1161.2}{T_s})$ |
| PS reactions | LH3 O{a} desorption | $O\{a\}(s) \rightarrow O(g) + (s)$ | $0.050457 T^2 \exp\left(-\frac{3177.2}{T_s}\right)$ |
| | LH3 CO{a} desorption | $CO\{a\}(s) \rightarrow CO(g) + (s)$ | $4485.5 \exp\left(-\frac{1581.4}{T_s}\right)$ |
| | LH3 CO{b} desorption | $CO\{b\}(s) \rightarrow CO(g) + (s)$ | $1.2194 \exp\left(-\frac{2251.6}{T_s}\right)$ |

[7] K. Swaminathan-Gopalan *et al.*, "**Development and validation of a finite-rate model for carbon oxidation by atomic oxygen.**" Carbon 137 (2018): 313-332.

Vitreous Carbon (VC) Oxidation Model





Effective models for use in CFD: Extension of VC model to FiberForm®



Objectives:

- Develop a predictive model of carbon oxidation for use in CFD

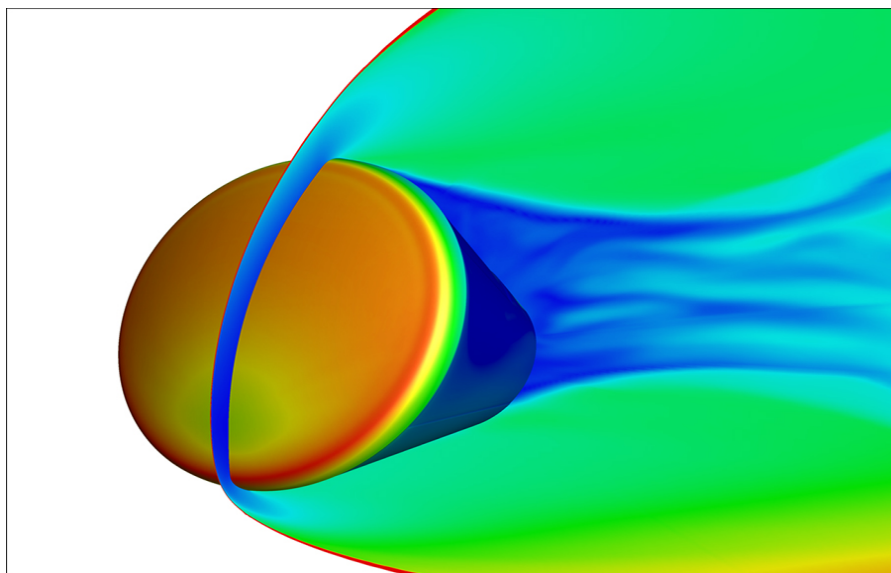
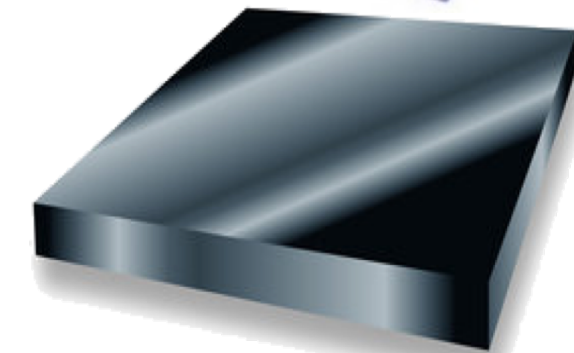
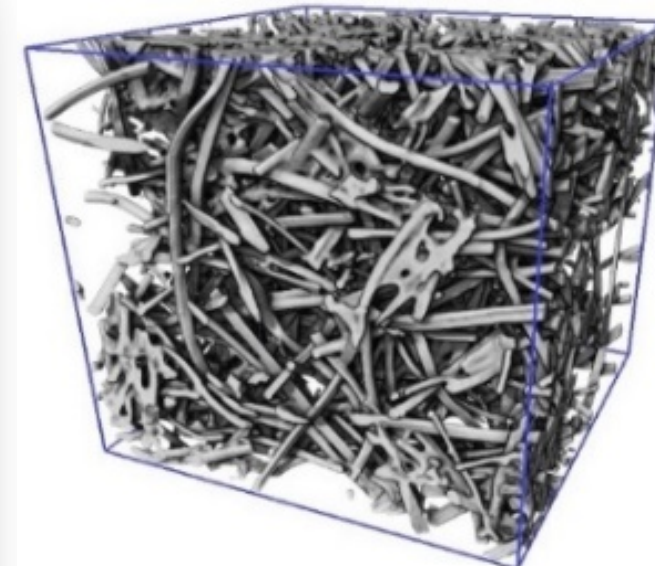


Image credit: NASA

FiberForm®



Vitreous carbon

Artist rendering.
Credit: SPI Supplies Division
of Structure Probe, Inc

Effective model for use in CFD

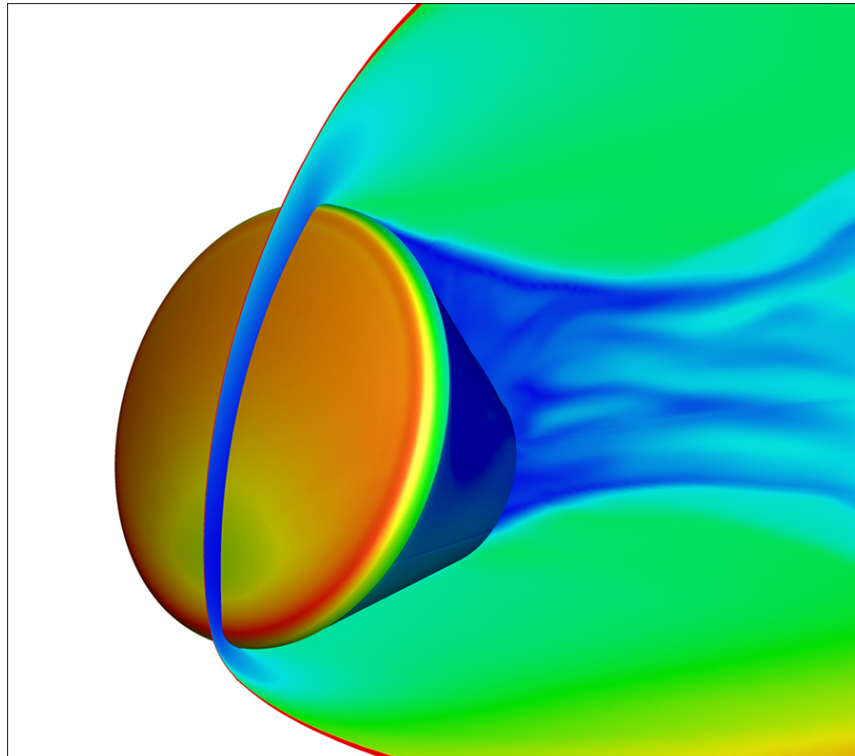
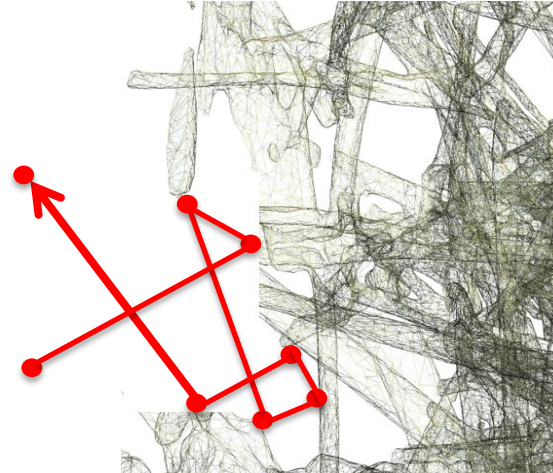
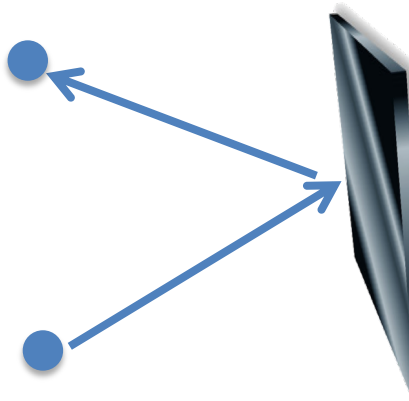


Image credit: NASA



Real model
Rates $\rightarrow k$

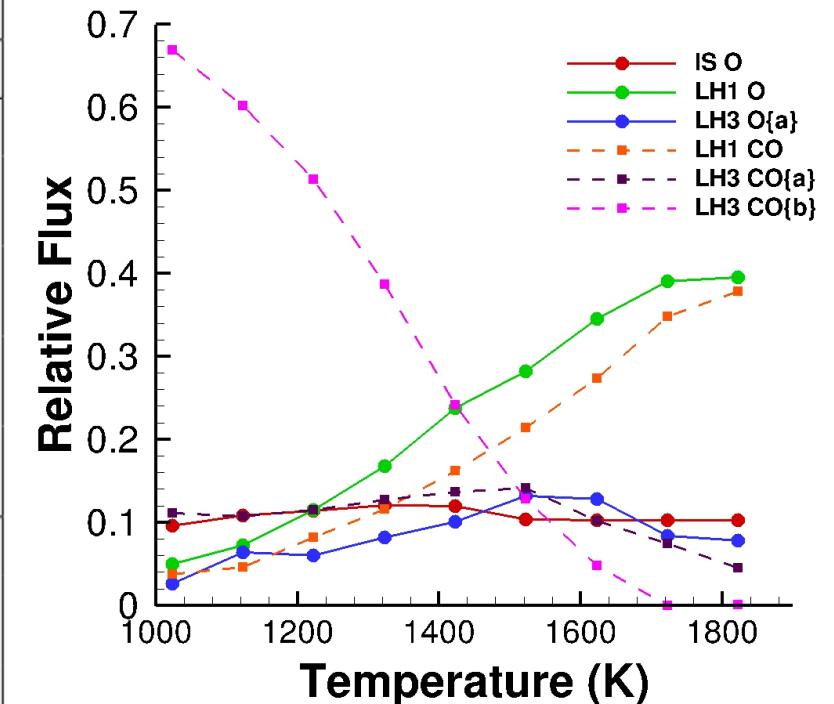


Effective model
Rates $\rightarrow k_{\text{eff}}$

Effective model for use in CFD



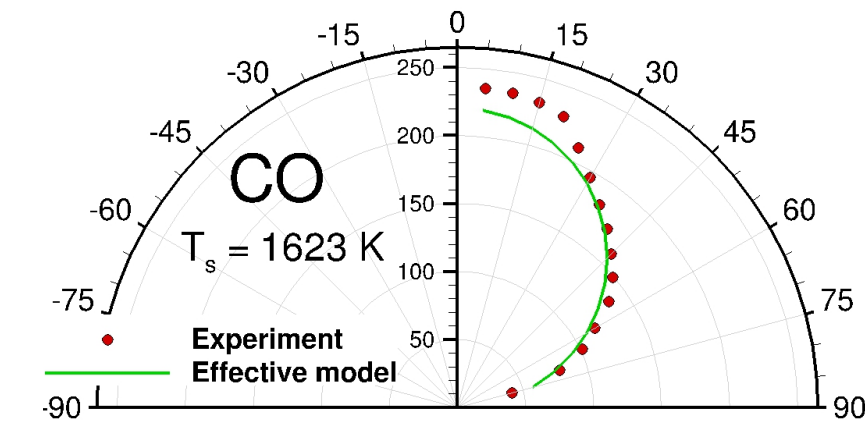
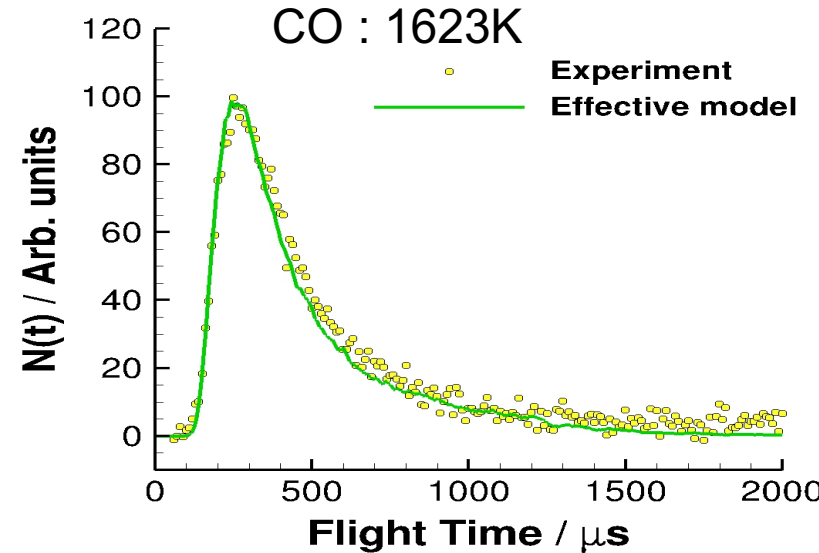
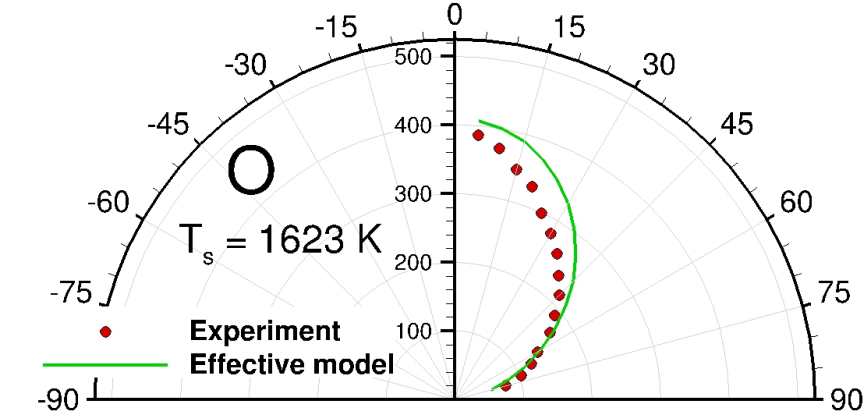
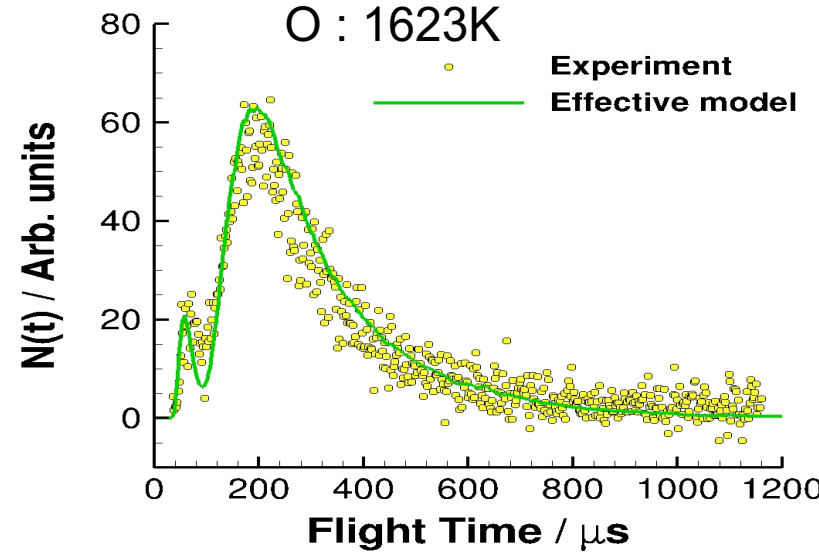
| Type | Mechanisms | Reaction |
|--------------|----------------------|---|
| Adsorption | Adsorption | $O(g) + (s) \rightarrow O(ads)$ |
| GS reactions | LH1 O formation | $O(ads) \rightarrow O(TD)(g) + (s)$ |
| | LH1 CO formation | $O(ads) + C(b) + O'(ads) \rightarrow CO(g) + (s) + O'(ads)$ |
| | LH3 O{a} formation | $O(ads) \rightarrow O\{a\}(s)$ |
| | LH3 CO{a} formation | $O(ads) + C(b) + O'(ads) \rightarrow CO\{a\}(s) + O'(ads)$ |
| | LH3 CO{b} formation | $O(ads) + C(b) + O'(ads) \rightarrow CO\{b\}(s) + O'(ads)$ |
| PS reactions | LH3 O{a} desorption | $O\{a\}(s) \rightarrow O(g) + (s)$ |
| | LH3 CO{a} desorption | $CO\{a\}(s) \rightarrow CO(g) + (s)$ |
| | LH3 CO{b} desorption | $CO\{b\}(s) \rightarrow CO(g) + (s)$ |



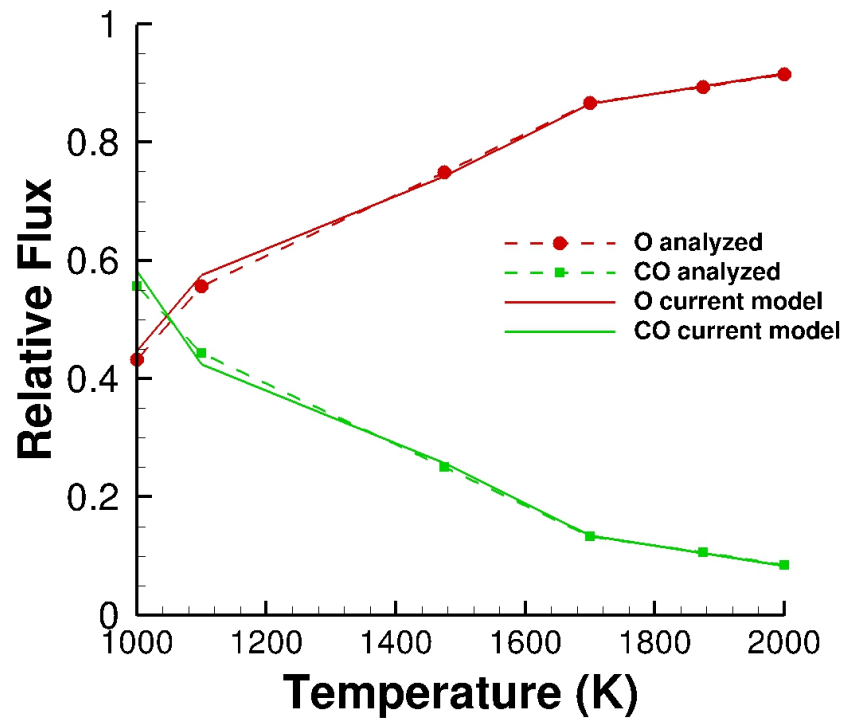
Effective model for use in CFD



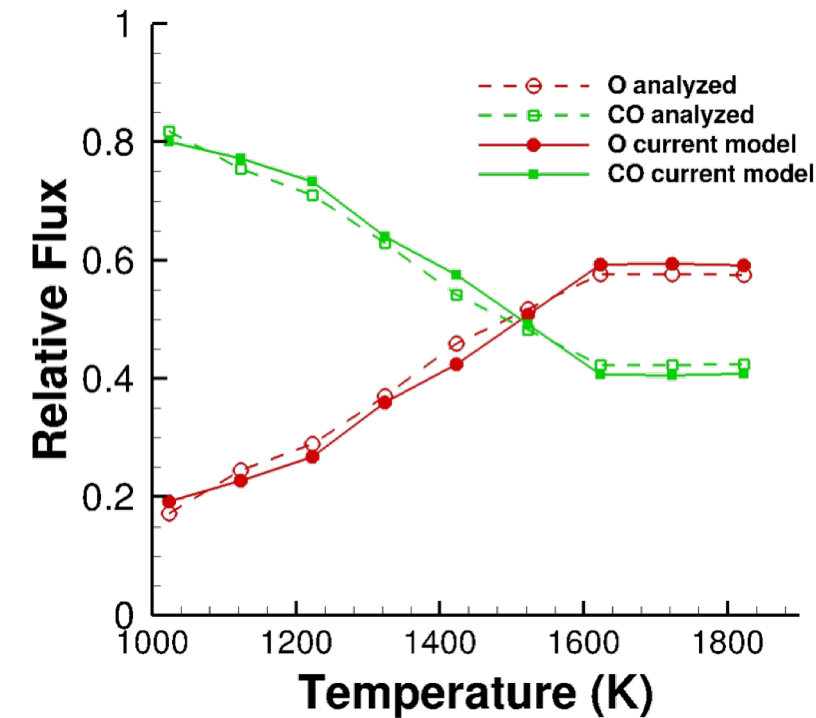
| Type | Mechanisms | Reaction | Rate constant (k) |
|--------------|----------------------|---|--|
| Adsorption | Adsorption | $O(g) + (s) \longrightarrow O(ads)$ | $\frac{1}{\Phi} * \frac{1}{4} \sqrt{\frac{8k_b T_a}{\pi m}} * 0.892$ |
| | LH1 O formation | $O(ads) \longrightarrow O(TD)(g) + (s)$ | $7.85 \exp(-\frac{5154.6}{T_s})$ |
| | LH1 CO formation | $O(ads) + C(b) + O'(ads) \longrightarrow CO(g) + (s) + O'(ads)$ | $\frac{1}{\Phi} * 964555.3 \exp(-\frac{16574.0}{T_s})$ |
| | LH3 O{a} formation | $O(ads) \longrightarrow O\{a\}(s)$ | 1 |
| | LH3 CO{a} formation | $O(ads) + C(b) + O'(ads) \longrightarrow CO\{a\}(s) + O'(ads)$ | $\frac{1}{\Phi} * 8337.8 \exp(-\frac{10360.8}{T_s})$ |
| GS reactions | LH3 CO{b} formation | $O(ads) + C(b) + O'(ads) \longrightarrow CO\{b\}(s) + O'(ads)$ | $\frac{1}{\Phi} * 57.83 \exp(-\frac{2908.9}{T_s})$ |
| | LH3 O{a} desorption | $O\{a\}(s) \longrightarrow O(g) + (s)$ | $0.05 T^2 \exp\left(-\frac{3177.2}{T_s}\right)$ |
| | LH3 CO{a} desorption | $CO\{a\}(s) \longrightarrow CO(g) + (s)$ | $4485.5 \exp\left(-\frac{1581.4}{T_s}\right)$ |
| PS reactions | LH3 CO{b} desorption | $CO\{b\}(s) \longrightarrow CO(g) + (s)$ | $1.2 \exp\left(-\frac{2251.6}{T_s}\right)$ |



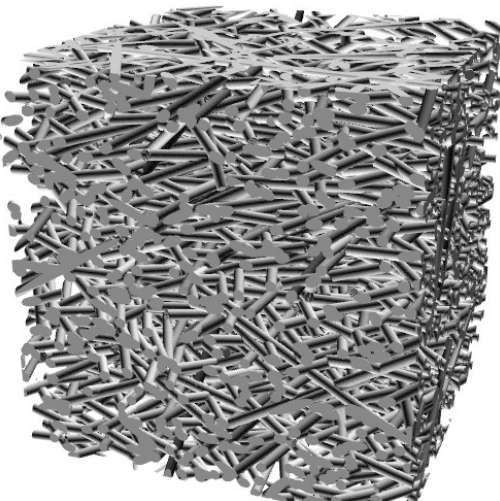
Vitreous Carbon model



Effective model



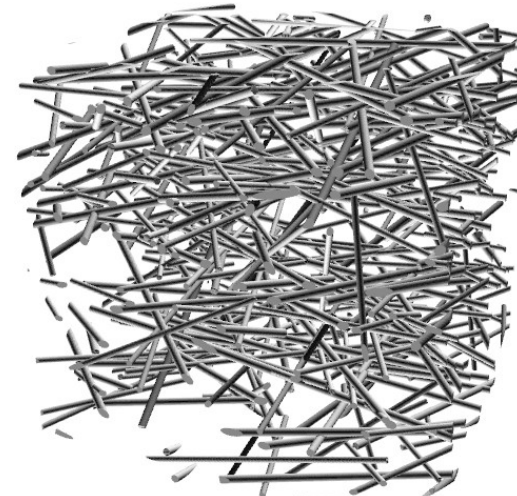
Varying porosity



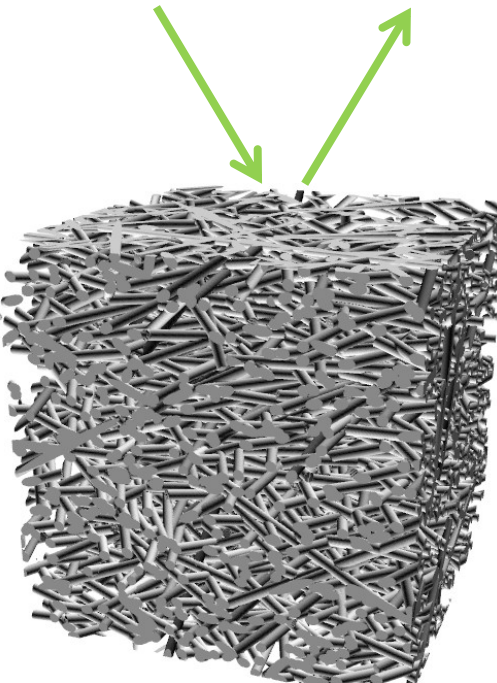
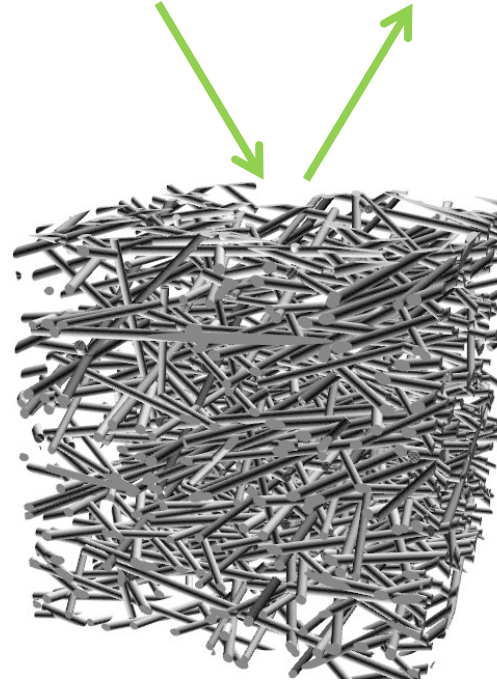
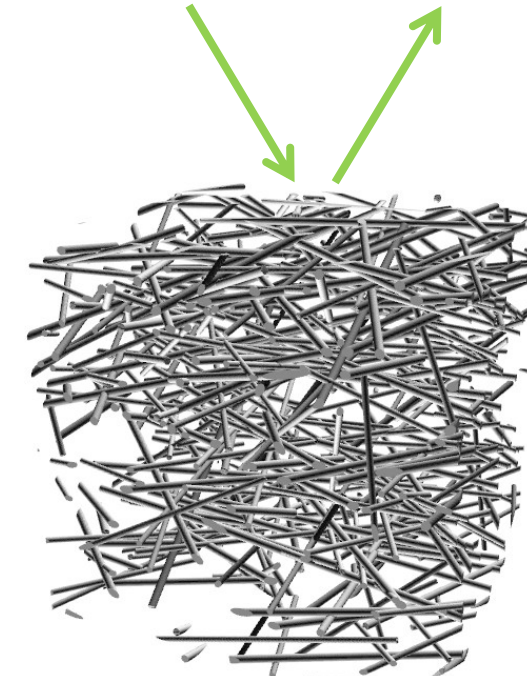
$$\phi = 0.84$$



$$\phi = 0.90$$



$$\phi = 0.96$$

Real model Rates → k**Effective Rates → $k_{\text{eff}}(T)$** **Effective Rates → $k_{\text{eff}}(T)$** **Effective Rates → $k_{\text{eff}}(T)$** **Effective model Rates → $k_{\text{eff}}(T, \phi)$**

FiberForm – Varying Porosity



| Mechanisms | Reaction | Rate constant $k = f(\Phi) * A * \exp(-E/T)$ | | | | |
|---------------------|---|--|---|-----------|-----------|-----------|
| | | $f(\Phi)$ | $A = a_0 + a_1 * \epsilon^1 + a_2 * \epsilon^2$ | | | E |
| | | | a_0 | a_1 | a_2 | |
| Adsorption | $O(g) + (s) \longrightarrow O(ads)$ | $\frac{1}{\Phi} * \frac{1}{4} \sqrt{\frac{8k_b T_g}{\pi m}}$ | +1.335E-1 | +1.583E+0 | -8.177E-1 | 0 |
| LH3 O{a} formation | $O(ads) \longrightarrow O\{a\}(s)$ | 1 | 1 | 0 | 0 | 0 |
| LH3 CO{a} formation | $O(ads) + C(b) + O'(ads) \longrightarrow CO\{a\}(s) + O'(ads)$ | $\frac{1}{\Phi}$ | -7.343E+4 | +1.636E+5 | -7.997E+4 | +1.036E+4 |
| LH3 CO{b} formation | $O(ads) + C(b) + O'(ads) \longrightarrow CO\{b\}(s) + O'(ads)$ | $\frac{1}{\Phi}$ | -5.093E+2 | +1.134E+3 | -5.547E+2 | +2.909E+3 |
| LH1 O formation | $O(ads) \longrightarrow O(TD)(g) + (s)$ | 1 | +6.298E+1 | -1.151E+2 | +5.943E+1 | +6.155E+3 |
| LH1 CO formation | $O(ads) + C(b) + O'(ads) \longrightarrow CO(g) + (s) + O'(ads)$ | $\frac{1}{\Phi}$ | -8.495E+6 | +1.892E+7 | -9.251E+6 | +1.657E+4 |

Conclusions

- Detailed surface chemistry framework was implemented in PuMA.
- The vitreous carbon (VC) model was extended to FiberForm® and validated.
- Effective oxidation model as a function of structural properties and temperature $k_{\text{eff}}(T, \Phi)$ was developed for use in CFD.

Future Work

- Extension to other species (N)